Bilel Hamil*, Houcine Aounallah and Bekir Can Lütfüoğlu

Graphene in curved Snyder space

https://doi.org/10.1515/zna-2020-0159
Received June 15, 2020; accepted July 28, 2020; published online September 18, 2020

Abstract: The Snyder-de Sitter (SdS) model which is invariant under the action of the de Sitter group, is an example of a noncommutative space-time with three fundamental scales. In this paper, we considered the massless Dirac fermions in graphene layer in a curved Snyder space-time which are subjected to an external magnetic field. We employed representation in the momentum space to derive the energy eigenvalues and the eigenfunctions of the system. Then, we used the deduced energy function obtaining the internal energy, heat capacity, and entropy functions. We investigated the role of the fundamental scales on these thermal quantities of the graphene layer. We found that the effect of the SdS model on the thermodynamic properties is significant.

Keywords: curved Snyder space; graphene; partition function; Snyder model; thermodynamic functions.

1 Introduction

Recently, an increasing interest is dedicated to the study of classical and quantum mechanics on a quantized space-time [1–10]. Historically Hartland S. Snyder was the pioneer of this idea. In 1947, he proposed a fundamental length and stated noncommutative operators of the quantized space-time coordinates with four translation generators of the algebra [11]. Originally, this attempt was solely aimed to solve the problems connected to ultraviolet (UV) divergences in quantum field theory. In the same year, he published a second article in which he discussed the effect of quantized space-time on the electromagnetic field theory [12]. However, this article was his last published article on this subject. Meanwhile, due to the development of renormalization techniques, the UV divergences problem in quantum field theory has resolved. For this reason, Snyder's idea was not used more than some articles [13–18]. The curved space selected by Snyder is the (3+1) de Sitter space, fabricated as the homogeneous space:

$$dS^{(3+1)} = G/H = SO(4,1)/SO(3,1), \tag{1}$$

where $SO(4,1)$ is the group of isometriesf, $H = SO(3,1)$ is the Lorentz group while the Snyder-Galilean models are achieved as the nonrelativistic limit of the Snyder–Lorentzian models. The relativistic modified quantum algebra proposed by Snyder is based on the following commutation relations:

$$[X_\mu ; P_\nu] = i\hbar\left(\eta_{\mu\nu} + \beta P_\mu P_\nu\right); \quad [X_\mu ; X_\nu] = i\hbar\beta J_{\mu\nu}; \quad [P_\mu ; P_\nu] = 0. \tag{2}$$

Here, $\eta_{\mu\nu}$ is the metric tensor where its signature is $[\eta_{\mu\nu}] = \mathrm{diag}(-1111)$. β is a coupling constant proportional to the Planck length, $J_{\mu\nu}$ are the generators of Lorentz transformations, while μ and ν are the space-time indices with $\mu, \nu = 0, 1, 2, 3$. Via the presence of a fundamental constant, β, the model is seen to be an example of doubly (or deformed) special relativity [19]. Depending on the positive or negative values of the beta parameter, the model is called as Snyder and anti-Snyder model, respectively [2].

In 1947, in order to make Snyder's theory invariant under the group of translations that are based on the conformal group $SO(1,5)$, Yang extended Snyder's model to a de Sitter space-time background [13]. The resulting model is characterized by three invariant scales, the speed of light in vacuum, c, the Snyder parameter β, and the cosmological constant Λ. Therefore sometimes, that model is preferred to be named as triply special relativity instead of the Snyder-de Sitter (SdS) model. In momentum space a one-to-one correspondence between the Snyder/anti-Snyder model and the de Sitter/anti-de Sitter space-time is reported in a study by Guo et al. [20].

The SdS model's algebra is constructed with the position X_μ, momentum P_μ and Lorentz generator $J_{\mu\nu}$ operators, which obey the following algebra [21, 22].

***Corresponding author: Bilel Hamil,** Département de TC de SNV, Université Hassiba Benbouali, Chlef, Algeria,
E-mail: hamilbilel@gmail.com. https://orcid.org/0000-0002-7043-6104
Houcine Aounallah, Department of Science and Technology, Larbi Tebessi University, 12000 Tebessa, Algeria
Bekir Can Lütfüoğlu, Department of Physics, Akdeniz University, Campus 07058, Antalya, Turkey; Department of Physics, University of Hradec Králové, Rokitanského 62, 500 03 Hradec Králové, Czechia

$$
\begin{aligned}
\left[J_{\mu\nu}\,;X_\sigma\right] &= i\hbar\left(\eta_{\mu\sigma}X_\nu - \eta_{\nu\sigma}X_\mu\right);\\
\left[J_{\mu\nu}\,;P_\sigma\right] &= i\hbar\left(\eta_{\mu\sigma}P_\nu - \eta_{\nu\sigma}P_\mu\right),\\
\left[X_\mu\,;P_\nu\right] &= i\hbar\Big(\eta_{\mu\nu} + \alpha X_\mu X_\nu + \beta P_\mu P_\nu\\
&\quad + \sqrt{\alpha\beta}\left(P_\mu X_\nu + X_\nu P_\nu - J_{\mu\nu}\right)\Big),\\
\left[X_\mu\,;X_\nu\right] &= i\beta\hbar J_{\mu\nu}\,;\quad \left[P_\mu\,;P_\nu\right] = i\alpha\hbar J_{\mu\nu}.
\end{aligned}
\tag{3}
$$

This algebra can be regarded as a nonlinear realization of Yang model. It should be noted that α and β are the coupling constants with dimension of inverse length and inverse mass, they are defined as the square root of the cosmological constant $\sqrt{\alpha}\sim 10^{-24}\mathrm{cm}^{-1}$ and with mass of Planck $\sqrt{\beta}\sim 10^{5}\mathrm{g}^{-1}$ [19]. In the limits $\alpha\to 0$, and $\beta\to 0$ the algebra (3) reduces to the Snyder model in flat space and to the de Sitter algebra, respectively [23, 24]. The SdS phase space can be realized in six-dimensional space as $SO(1,5)/SO(1,3)\times O(2)$ if $\alpha,\beta>0$ and $SO(2,4)/SO(1,3)\times O(2)$ if $\alpha,\beta<0$ [5]. Recently, many authors have condensed their studies on the discussions over the deformed canonical commutation relations [5, 25–36].

In the last decade, Graphene has attracted the attention of theoretical and experimental physicists [37–39]. A graphene material has a two-dimensional structure that is constituted from carbon atoms in the honeycomb lattice form which yields superior mechanical properties in addition to optical and electronic properties [40–43]. In the theoretical perspective, a low energy excitation in a single graphene layer is described by the massless Dirac equation [44, 45].

In this paper, we consider massless fermions located in a graphene layer under the effect of a perpendicular external magnetic field. We solve the Dirac equation in the SdS model and obtain the energy eigenvalue function. Then, we explore the thermodynamic functions in order to discuss the effects of the fundamental scales of the SdS model. We present the manuscript as follows: In section 2, we introduce the SdS model briefly. In section 3, we solve the massless Dirac equation. We obtain the energy spectrum function analytically. Next, in section 4 we define the partition function. At the high-temperature limit, first, we derive the internal energy functions, and then, the heat capacity and the entropy functions. We demonstrate the thermodynamic functions versus temperature and discuss the effect of the fundamental coupling constants of the SdS model. We end the manuscript with a brief conclusion.

2 Curved Snyder model

In the nonrelativistic curved Snyder model, the modified commutation relations between the position and momentum operators are given by [22, 36]:

$$
\begin{aligned}
\left[X_j\,;P_k\right] &= i\hbar\Big(\delta_{jk} + \alpha X_jX_k + \beta P_jP_k + \sqrt{\alpha\beta}\left(P_jX_k + X_kP_j\right)\Big),\\
\left[X_j\,;X_k\right] &= i\beta\hbar J_{jk},\quad \left[P_j\,;P_k\right] = i\alpha\hbar J_{jk},
\end{aligned}
\tag{4}
$$

where $J_{jk} = (X_jP_k - X_kP_j)$. In [22, 36], one set of the X_j and P_j operators which satisfies the algebra is expressed in the canonical coordinates as

$$
X_j = \mathcal{X}_j + \lambda\sqrt{\frac{\beta}{\alpha}}\mathcal{P}_j = i\hbar\sqrt{1-\beta p^2}\;\frac{\partial}{\partial p_j} + \lambda\sqrt{\frac{\beta}{\alpha}}\;\frac{p_j}{\sqrt{1-\beta p^2}},
\tag{5}
$$

$$
\begin{aligned}
P_j &= -\sqrt{\frac{\alpha}{\beta}}\mathcal{X}_j + (1-\lambda)\mathcal{P}_j\\
&= -i\hbar\sqrt{\frac{\alpha}{\beta}}\sqrt{1-\beta p^2}\;\frac{\partial}{\partial p_j} + (1-\lambda)\frac{p_j}{\sqrt{1-\beta p^2}}.
\end{aligned}
\tag{6}
$$

Here, λ is an arbitrary real parameter. Note that p_j is bounded in the range of $-\frac{1}{\sqrt{\beta}} < p_j < \frac{1}{\sqrt{\beta}}$. If we consider a case, where $(\langle P_j\rangle = \langle X_j\rangle = 0)$, we obtain the uncertainty relation as

$$
\begin{aligned}
(\Delta X)_j(\Delta P)_k \geq \frac{\hbar}{2}\Big(&\delta_{jk} + \alpha(\Delta X)_j(\Delta X)_k + \beta(\Delta P)_j(\Delta P)_k\\
&- \sqrt{\alpha\beta}\left((\Delta P)_j(\Delta X)_k + (\Delta X)_j(\Delta P)_k\right)\Big).
\end{aligned}
\tag{7}
$$

In one dimension case, Eq. (7) reduces to

$$
(\Delta X)(\Delta P) \geq \frac{\hbar}{2}\,\frac{\left(1+\alpha(\Delta X)^2 + \beta(\Delta P)^2\right)}{1+\hbar\sqrt{\alpha\beta}}.
\tag{8}
$$

As a conclusion, the modification in the algebra produces the following minimal uncertainties in both position and momentum measurements

$$
\begin{aligned}
(\Delta X)_{\min} &= \frac{\hbar\sqrt{\beta}}{\sqrt{1+2\hbar\sqrt{\alpha\beta}}} \sim \hbar\sqrt{\beta}\,;\\
(\Delta P)_{\min} &= \frac{\hbar\sqrt{\alpha}}{\sqrt{1+2\hbar\sqrt{\alpha\beta}}} \sim \hbar\sqrt{\alpha}.
\end{aligned}
\tag{9}
$$

We note that, if $\alpha, \beta < 0$ minimal uncertainties do not emerge and all real values of P_i are allowed. Before we proceed through the next section, it is worth remarking the change of the definition of the scalar product with the following form of [22],

$$\langle\varphi|\psi\rangle = \int \frac{d^3p}{\sqrt{1-\beta p^2}}\varphi^*(p)\psi(p). \tag{10}$$

3 Graphene in an external magnetic field

In this section, we solve the (2+1)-dimensional massless Dirac equation in the curved Snyder model in the presence of the uniform magnetic field B, which is directed along the z axis. We assume $B > 0$ and employ $A = \frac{B}{2}(-X_2, X_1)$ gauge. We start with the Dirac equation

$$i\hbar\frac{\partial}{\partial t}\Psi = H\Psi. \tag{11}$$

Here, ψ is a two-dimensional wave function that describes the electron states between the two Dirac points A and B, while the Dirac Hamiltonian is

$$H = V_F\vec{\alpha}\cdot\left(\vec{P} - \frac{e}{c}\vec{A}\right), \tag{12}$$

where $V_F = (1.12 \pm 0.02)\times10^6$ ms^{-1} is the Fermi velocity. We define a fundamental length scale, ℓ_B, in the presence of an external magnetic field via $\ell_B = \sqrt{\frac{\hbar c}{eB}}$, and express the Hamiltonian in the matrix form

$$H = \begin{pmatrix} H_A & 0 \\ 0 & H_B \end{pmatrix}, \tag{13}$$

with two Hamiltonian operators for the two Dirac points A and B as

$$H_A = V_F\begin{pmatrix} 0 & (P_1 - iP_2) + \frac{\hbar}{2\ell_B^2}(X_2 + iX_2) \\ (P_1 + iP_2) + \frac{\hbar}{2\ell_B^2}(X_2 - iX_2) & 0 \end{pmatrix}, \tag{14}$$

$$H_B = V_F\begin{pmatrix} 0 & (P_1 + iP_2) + \frac{\hbar}{2\ell_B^2}(X_2 - iX_2) \\ (P_1 - iP_2) + \frac{\hbar}{2\ell_B^2}(X_2 + iX_2) & 0 \end{pmatrix}. \tag{15}$$

We write the two-component wave function as

$$\Psi = e^{\frac{iE}{\hbar}t}\begin{pmatrix} \psi^A \\ \psi^B \end{pmatrix}, \tag{16}$$

where ψ^A and ψ^B are two-dimensional eigenstates. To obtain the energy eigenvalue equation of the wave function at the Dirac point A, we solve the following system of two coupled equations:

$$\left[P_1 - iP_2 + \frac{\hbar}{2\ell_B^2}(X_2 + iX_1)\right]\psi^B = \frac{E}{V_F}\psi^A, \tag{17}$$

$$\left[P_1 + iP_2 + \frac{\hbar}{2\ell_B^2}(X_2 - iX_1)\right]\psi^A = \frac{E}{V_F}\psi^B. \tag{18}$$

Out of the coupled system, we obtain the following decoupled differential equation for the component ψ^A.

$$\begin{aligned}&\left[P_1^2 + P_2^2 + \left(\frac{\hbar}{2\ell_B^2}\right)^2\left(X_2^2 + X_1^2\right) + i[P_1\,;P_2]\right.\\ &+i\left(\frac{\hbar}{2\ell_B^2}\right)^2[X_1\,;X_2] + \frac{\hbar}{2\ell_B^2}(P_1X_2 + X_2P_1 - X_1P_2 - P_2X_1)\\ &\left.+\frac{i\hbar}{2\ell_B^2}[X_1\,;P_1] + \frac{i\hbar}{2\ell_B^2}\Big[X_2\,;P_2\Big]\right]\psi^A = \frac{E^2}{V_F{}^2}\psi^A.\end{aligned} \tag{19}$$

Then, we employ the position and momentum operators given in Eqs. (5) and (6). We find

$$\begin{aligned}&\left\{\left[\frac{\beta}{\alpha}\left(\frac{\hbar}{2\ell_B^2}\right)^2 + 1\right]\left(\sqrt{\frac{\alpha}{\beta}}\mathcal{X}_j\right)^2\right.\\ &+\left(1 - 2\lambda + \lambda^2\left[\frac{\beta}{\alpha}\left(\frac{\hbar}{2\ell_B^2}\right)^2 + 1\right]\right)\mathcal{P}_j^2 - \left[\frac{\beta}{\alpha}\left(\frac{\hbar}{2\ell_B^2}\right)^2 + 1\right]\alpha\hbar L_z\\ &-\left(1 - \lambda\left[\frac{\beta}{\alpha}\left(\frac{\hbar}{2\ell_B^2}\right)^2 + 1\right]\right)\sqrt{\frac{\alpha}{\beta}}(\mathcal{X}_j\mathcal{P}_j + \mathcal{P}_j\mathcal{X}_j)\\ &\left.-\frac{\hbar^2}{\ell_B^2}\left(1 + \frac{L_z}{\hbar} + \frac{\beta}{2}\mathcal{P}_j^2\right)\right\}\psi^A = \frac{E^2}{V_F{}^2}\psi^A.\end{aligned} \tag{20}$$

In order to simplify the differential equation we assume

$$\lambda = \left[\frac{\beta}{\alpha}\left(\frac{\hbar}{2\ell_B^2}\right)^2 + 1\right]^{-1} \tag{21}$$

Then, $(\mathcal{X}_j\mathcal{P}_j + \mathcal{P}_j\mathcal{X}_j)$ term vanishes and Eq. (20) becomes

$$\left\{-(1-\beta p^2)\left(\frac{\partial^2}{\partial p^2}+\frac{1}{p}\frac{\partial}{\partial p}-\frac{\mu^2}{p^2}\right)+\beta p\frac{\partial}{\partial p}+\frac{1}{2\ell_{\mathcal{B}}^2}\left(\frac{1}{2\ell_{\mathcal{B}}^2}-1\right)\frac{\beta^2p^2}{1-\beta p^2}-\beta\mu-\frac{\beta}{\ell_{\mathcal{B}}^2}(\mu+1)\right\}\Phi^A=\frac{\beta\mathcal{E}^2}{\hbar^2{V_F}^2}\Phi^A, \tag{22}$$

where

$$\psi^A=\frac{e^{i\mu\varphi}}{\sqrt{2\pi}}\Phi^A;\quad(\mu=0,\pm1,\pm2,\ldots), \tag{23}$$

and

$$\frac{1}{\ell_{\mathcal{B}}^2=\frac{\alpha}{\lambda}\frac{1}{\ell_B^2}};\quad \mathcal{B}\equiv\frac{\lambda B}{\alpha};\quad \mathcal{E}^2\equiv\frac{\lambda E^2}{\alpha}. \tag{24}$$

We perform a change of the variable

$$\rho=\frac{\sin^{-1}\sqrt{\beta}p}{\sqrt{\beta}}, \tag{25}$$

which maps the allowed range from $\frac{-1}{\sqrt{\beta}}<p<\frac{1}{\sqrt{\beta}}$ to $\frac{-\pi}{2\sqrt{\beta}}<\rho<\frac{\pi}{2\sqrt{\beta}}$. Equation (22) reduces to the form of

$$\left[\frac{\partial^2}{\partial\rho^2}+\sqrt{\beta}\cot\left(\sqrt{\beta}\rho\right)\frac{\partial}{\partial\rho}-\beta\mu^2\cot^2\left(\sqrt{\beta}\rho\right)-\frac{\beta}{2\ell_{\mathcal{B}}^2}\left(\frac{1}{2\ell_{\mathcal{B}}^2}-1\right)\tan^2\left(\sqrt{\beta}\rho\right)+\beta\mu+\frac{\beta(\mu+1)}{\ell_{\mathcal{B}}^2}+\frac{\beta\mathcal{E}^2}{\hbar^2{V_F}^2}\right]\Phi^A=0. \tag{26}$$

By ansatz, we assume $\Phi^A=\sin^{\mu}(\sqrt{\beta}\rho)\cos^{\delta}(\sqrt{\beta}\rho)\mathrm{F}$. Then, Eq. (26) becomes

$$\left\{\frac{\partial^2}{\partial\rho^2}+\sqrt{\beta}\left[(1+2\mu)\cot\left(\sqrt{\beta}\rho\right)-2\delta\tan\left(\sqrt{\beta}\rho\right)\right]\frac{\partial}{\partial\rho}+\beta\left[\delta(\delta-1)-\frac{1}{2\ell_{\mathcal{B}}^2}\left(\frac{1}{2\ell_{\mathcal{B}}^2}-1\right)\right]\tan^2\left(\sqrt{\beta}\rho\right)+\left(\frac{1}{\ell_{\mathcal{B}}^2}-2\delta\right)\beta(\mu+1)+\frac{\beta\mathcal{E}^2}{\hbar^2{V_F}^2}\right\}\mathrm{F}=0 \tag{27}$$

We fix the parameter δ by requiring the coefficient of the $\tan^2(\sqrt{\beta}\rho)$ to vanish:

$$\delta(\delta-1)-\frac{1}{2\ell_{\mathcal{B}}^2}\left(\frac{1}{2\ell_{\mathcal{B}}^2}-1\right)=0. \tag{28}$$

We determine the roots of the quadratic equation of δ as

$$\delta=\frac{1}{2\ell_{\mathcal{B}}^2};\quad \delta'=1-\frac{1}{2\ell_{\mathcal{B}}^2}. \tag{29}$$

We note that the second root does not lead to a physically acceptable wave function unless we impose the condition $\ell_{\mathcal{B}}^2>1/2$. However, this condition is valid only for small enough field strengths. Therefore, we use the first root in Eq. (29). We find the reduced equation in the form of

$$\left[\frac{\partial^2}{\partial\rho^2}+\sqrt{\beta}\left[(1+2\mu)\cot\left(\sqrt{\beta}\rho\right)-2\delta\tan\left(\sqrt{\beta}\rho\right)\right]\frac{\partial}{\partial\rho}+\frac{\beta\mathcal{E}^2}{\hbar^2{V_F}^2}\right]\mathrm{F}=0. \tag{30}$$

We define a new variable $q=\sin^2(\sqrt{\beta}\rho)$. Then, Eq. (30) turns into the form of the hypergeometric equation [46].

$$\left[q(1-q)\frac{\partial^2}{\partial q^2}+\left[(1+\mu)-\left(\frac{3}{2}+\mu+\delta\right)q\right]\frac{\partial}{\partial q}+\frac{\mathcal{E}^2}{4\hbar^2{V_F}^2}\right]F=0. \tag{31}$$

This equation has a regular solution at $q=0$ that is written in terms of hypergeometric functions as

$$\mathrm{F}=\mathbf{F}(a,b,1+\mu;q), \tag{32}$$

with the following parameters:

$$\mathrm{a}=\frac{1}{4}+\frac{\delta+\mu}{2}+\frac{1}{2}\sqrt{\frac{1}{4}+\mu(1+\mu)+2\mu\delta+\delta(\delta+1)+\frac{\mathcal{E}^2}{\hbar^2{V_F}^2}}, \tag{33}$$

$$\mathrm{b}=\frac{1}{4}+\frac{\delta+\mu}{2}-\frac{1}{2}\sqrt{\frac{1}{4}+\mu(1+\mu)+2\mu\delta+\delta(\delta+1)+\frac{\mathcal{E}^2}{\hbar^2{V_F}^2}}. \tag{34}$$

The hypergeometric function $\mathbf{F}(a,b,c;q)$ is determined by the hypergeometric series [46] as follows:

$$\mathbf{F}(a,b,c,q)=\sum_{n=0}\frac{(a)_n(b)_n}{(c)_n}\frac{q^n}{n!}, \tag{35}$$

where the parameters of the hypergeometric series are given by

$$(a)_n=\frac{\Gamma(a+n)}{\Gamma(a)};\quad (b)_n=\frac{\Gamma(b+n)}{\Gamma(b)};\quad (c)_n=\frac{\Gamma(c+n)}{\Gamma(c)}. \tag{36}$$

The series reduces to a polynomial if a or b is a negative integer. Using the expressions of b, we finally obtain

$$E_n = \pm\hbar V_F\sqrt{4\theta n^2 + 2\theta n\left(1+\frac{1}{\ell_B^2\theta}+2\mu\right)}, \tag{37}$$

where $\theta = \alpha + \frac{\hbar^2\beta}{4\ell_B^4}$. We would like to emphasize that the latter equation represents the main result of our paper. We observe that the introduced deformed Heisenberg algebra has influence on results. We also note that the energy spectrum depends on n^2, which is a feature of hard confinement. Furthermore, the energy spectrum values increase proportional to n for the large quantum number n. It should be pointed out that for $n = 0$, the energy level $E_n = 0$, which means the energy level at higher levels ($n = 1, 2, \ldots$) are distributed symmetrically around $n = 0$. In addition, the energy level is proportional to $\sqrt{n^2}$, which implies the energy spacing between adjacent levels is not constant. For large n the energy spacing becomes constant

$$\lim_{n\to\infty}\Delta E_n = \left|E_{n+1} - E_n\right| = \hbar\omega_c, \tag{38}$$

where $\omega_c = 2V_F\sqrt{\theta}$ can be interpreted as classical cyclotron frequency. As α and β are small in comparison with the other quantities in the theory, we expand (37) to first order in α and β, we obtain

$$E_n = \pm\frac{\hbar V_F}{\ell_B}\sqrt{2n} \pm \theta\hbar V_F\sqrt{2n\left(n+\mu+\frac{1}{2}\right)^2}. \tag{39}$$

Here, the first term represent the Landau levels of electrons in graphene while the second term is the quantum gravity correction. Now, let us consider the following particular cases.

(1) In the limit $\beta \to 0$, we recover the results for anti-de Sitter space [47].

$$E_n = \pm\hbar V_F\sqrt{4\alpha n^2 + 2\alpha n(1+2\mu) + \frac{2n}{\ell_B^2}}. \tag{40}$$

(1) In the limit $\alpha \to 0$, we obtain the energy spectrum in the Snyder space.

$$E_n = \pm\hbar V_F\sqrt{\frac{\hbar^2\beta}{\ell_B^4}n^2 + \frac{\hbar^2\beta}{2\ell_B^4}n(1+2\mu) + \frac{2n}{\ell_B^2}}. \tag{41}$$

(1) In anti–Snyder-de Sitter model where $\alpha < 0$ and $\beta < 0$, the energy spectrum is,

$$E_n = \pm\hbar V_F\sqrt{\frac{2n}{\ell_B^2} - \left(\alpha + \frac{\hbar^2\beta}{4\ell_B^4}\right)[4n^2 + 2n(1+2\mu)]}. \tag{42}$$

in this case the energy spectrum E_n becomes complex when the quantum number n is large. This stipulates an upper bound on the allowed values of n.

(1) In the limit $\beta \to 0$ and $\alpha \to 0$, we get the ordinary quantum mechanical result [48, 49].

$$E_n = \pm\frac{\hbar V_F}{\ell_B}\sqrt{2n}. \tag{43}$$

(1) If $\delta = 1 - \frac{1}{2\ell_B^2}$, the energy spectrum is,

$$E_n = \pm\hbar V_F\sqrt{\theta}\sqrt{4n^2 + 4n\mu + 6n + 2\mu + 2 - (1+2\mu+2n)\frac{e\mathcal{B}}{\hbar c}}. \tag{44}$$

On another side, if a or b is a nonnegative integer, the hypergeometric series converges absolutely for all values of $|q| < 1$ [50] and,

$$\frac{(a)_n(b)_n}{(c)_n} = \frac{\Gamma(c)}{\Gamma(a)\Gamma(b)}n^{\delta-\frac{3}{2}}\left[1+\mathcal{O}(n^{-1})\right]. \tag{45}$$

For to make the hypergeometric function to be regular at $q = 1$, we must impose $\ell_B^2 > 1$, which is valid only for small enough field strengths. In the case where the particles cannot be bounded, only scattering solutions occur and the energy spectrum becomes continuous.

In order to demonstrate the influence of the modified algebra on the energy levels, we plot the energy levels $\epsilon = \frac{E_{n,\mu=0}}{\hbar V_F}$ versus the quantum number, n, by employing different values of the deformation parameters in Figure (1). We observe that the contribution of the α parameter is more significant than the β parameter.

It should be noted that the dependence of the energy levels on SdS parameters is only through θ, and this can be easily quantified. For weak magnetic fields, the parameter θ identified as the cosmological constant, θ~α~10^{-48}. If the

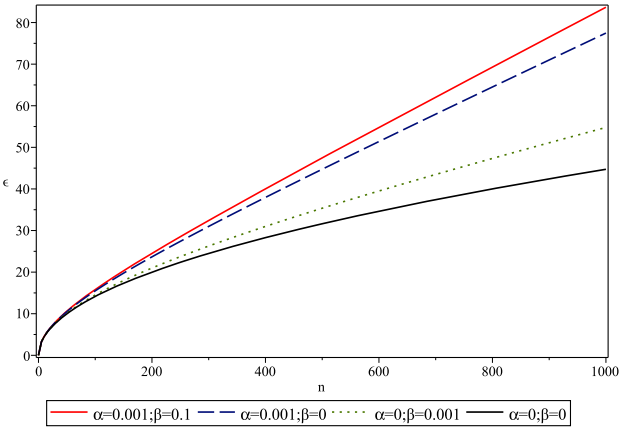

Figure 1: $\frac{E_{n,\mu=0}}{\hbar V_F}$ versus the quantum number n for different values of the deformation parameters.

magnetic field is extremely strong the parameter θ take the value $\theta \sim \frac{e^2B^2\beta}{c^2} \sim 10^{-44}B^2$.

4 Thermodynamic functions

It is a well-known fact that an electron gas obeys the Fermi–Dirac quantum statistic. However, in high temperatures or with the consideration of the electron gas in a low density, the Maxwell–Boltzmann statistic can be used instead [51]. In this section we aim to determine the thermodynamic properties of the of the graphene under a magnetic field in SdS space. We suppose only fermions with positive energy ($E \geq 0$) constitute the thermodynamic ensemble. Since we ignore the particle–particle interactions, we take neither negative-energy excited states nor the phenomenon of creation of particles into account [49, 52]. Therefore, we assume the partition function contains only a sum over positive-energy states. We note that this is an enormous simplification characteristic. We begin by computing the partition function of a single particle of the system, Z, for the fixed angular momentum ($\mu = 0$):

$$Z = \sum_{n=0}^{+\infty} e^{-\frac{E_n}{KT}}. \tag{46}$$

Here, K denotes the Boltzmann constant, T represents the thermodynamic temperature and E_n is the energy eigenvalues. We use the derived energy eigenvalue function given in Eq. (39) in Eq. (46). We obtain the partition function in the form of

$$Z = \sum_{n=0}^{+\infty} e^{-\frac{\hbar V_F}{KT}\sqrt{2\theta(2n^2+1)+\frac{2n}{\ell_B^2}}}. \tag{47}$$

Since α and β are small in comparison with the other quantities in the theory, we expand Eq. (47) till to the first order of α and β. We obtain

$$Z = \sum_{n=0}^{+\infty}\left[1-\frac{\hbar V_F\theta}{2}\sqrt{2n}-\frac{\hbar V_F\theta}{4}(2n)^{\frac{3}{2}}\right]e^{-\tilde{\beta}\sqrt{n}}, \tag{48}$$

where $\tilde{\beta} = \frac{1}{\tau}$, and τ is the reduced temperature defined with

$$\tau = \frac{KT\ell_B}{\hbar V_F\sqrt{2}} = \frac{T}{T_0}. \tag{49}$$

Here, $T_0 = \frac{\hbar V_F\sqrt{2}}{K\ell_B}$ is the temperature reference value, for instance when $B = 18T$, the value of this temperature becomes $T_0 = 3551$ K. It is worth noting that the first term in Eq. (48) is the ordinary partition function of the graphene under a magnetic field

$$Z_0 = \sum_{n=0}^{+\infty} e^{-\tilde{\beta}\sqrt{n}} = \frac{1}{\tilde{\beta}^2} + \zeta(0) = \frac{1}{\tilde{\beta}^2} - \frac{1}{2}. \tag{50}$$

We calculate the second and third terms of Eq. (48) by using the derivatives of Eq. (50) as follows:

$$\sum_{n=0}^{+\infty}\left[\frac{\hbar V_F\theta}{2}\sqrt{2n}+\frac{\hbar V_F\theta}{4}(2n)^{\frac{3}{2}}\right]e^{-\tilde{\beta}\sqrt{n}} = \left[-\frac{\hbar V_F\theta\sqrt{2}}{2}\frac{\partial}{\partial\tilde{\beta}}-\hbar V_F\theta\sqrt{2}\,\frac{\partial^3}{\partial\tilde{\beta}^3}\right]Z_0. \tag{51}$$

After all, we obtain the total partition function of the system in the SdS space in the form of

$$Z = \tau^2 - \frac{1}{2} - \hbar V_F\theta\sqrt{2}\tau^3(1+24\tau^2). \tag{52}$$

Next, we derive the thermal properties of our system, such as the internal energy and the specific heat through the numerical partition function Z via the following relations:

$$U = \frac{\ell_B}{\hbar V_F\sqrt{2}}\mathbf{U} = \tau^2\frac{\partial}{\partial\tau}\ln Z, \quad C = \frac{\partial U}{\partial\tau}. \tag{53}$$

We take $\ell_B = \hbar = c = K = 1$, and demonstrate all profiles of the thermodynamic quantities as a function of τ for various values of the SdS parameters.

First, we plot the partition function versus τ in Figure (2). We observe a monotonic increase in the partition function in the ordinary quantum mechanic limit. This characteristic behavior drastically changes in the existence of the SdS model parameters. We observe a decrease in the partition function while the temperature increases at the high-temperature values. The amount of the decrease in the partition function value increases when de Sitter spacetime is taken into account instead of the Snyder model.

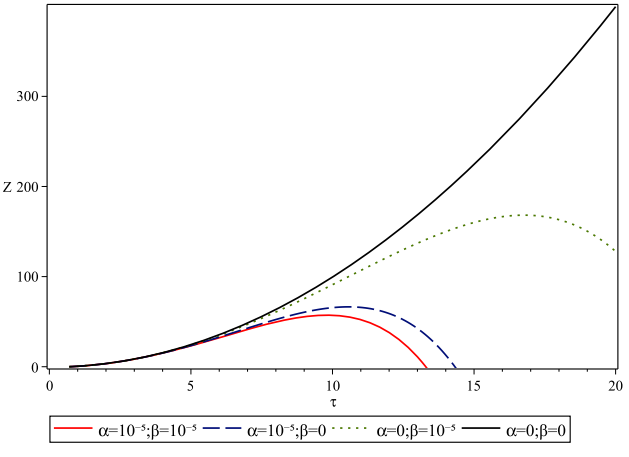

Figure 2: Partition function versus the reduced temperature.

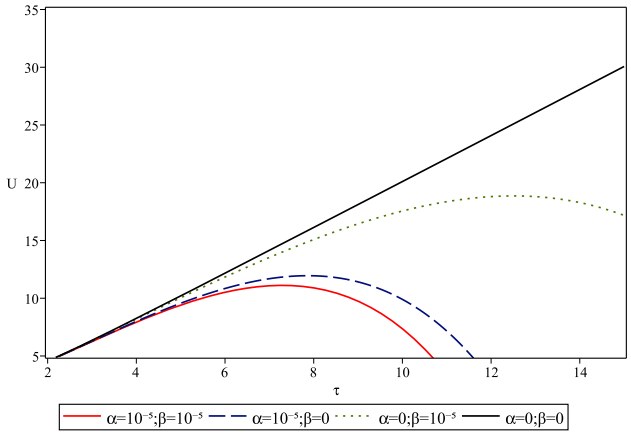

Figure 3: Internal energy versus the reduced temperature.

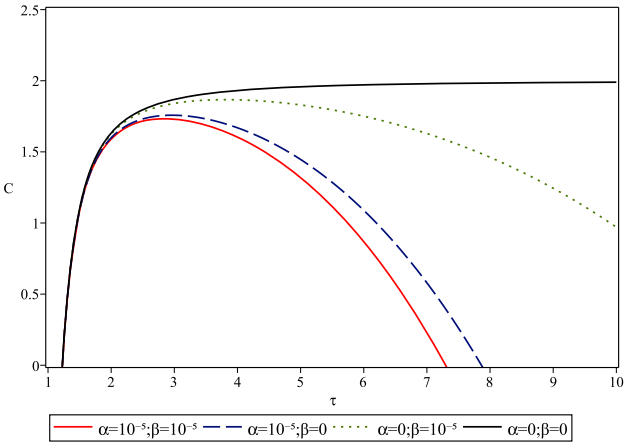

Figure 4: Specific heat function versus the reduced temperature.

We present the characteristic behavior of the internal energy function versus the dimensionless reduced temperature for different values of the SdS parameters in Figure (3). In the ordinary quantum mechanic limit, we observe a linear increase. When we consider a comparison between the role of the and parameters, we observe that the internal energy is being modified significantly in the de Sitter space, rather than the Snyder model because of the dependence on the strength of the magnetic field. We also see that in the vicinity of zero, there is no difference between the standard and the modified internal energy, which implies that the effects of quantum gravity become more obvious only at high temperatures.

Finally, we illustrate the heat capacity function versus the reduced temperature in Figure (4) by considering different values of the SdS parameters. In the ordinary quantum mechanic limit, we observe that the heat capacity will tend to a constant value at high temperature. We also see a decrease in the heat capacity function for high-temperature in the existence of (α, β). When we consider a comparison in between the parameters, like the other cases, we realize that the role of the parameter α is more significant than the β parameter.

It is worthwhile to note that all thermodynamic quantities obtained numerically in our work show that the effects of the curved Snyder model on the statistical properties of graphene are important only in the high-temperature regime, contrary the case at low temperatures. The effect of the SdS model becomes insignificant and the curves join rapidly as the temperature decreases. Our conclusion that the quantum gravity effects have concrete effects specifically at high-temperature limits.

Finally, when SdS parameters $\alpha = \beta = 0$ our results agrees exactly with that of [48]. One of the biggest issues in physics at present is to combine the quantum theory and the theory of general relativity into a unified framework, different approaches toward such a theory of quantum gravity have been elaborated. Despite that, one major obstacle is the absence of experimental confirmation of quantum gravitational effects [53]. The results we presented here may afford a source of information to probing Planck-scale physics in future experiments.

5 Conclusion

In this paper, we considered a graphene layer which is under the influence of an external magnetic field. We assumed the applied field to be perpendicular to the layer and solved the massless Dirac equation in the (2+1) dimension in the SdS model. We derived an analytic solution to the wave and energy eigenvalue functions. The essential characteristic of energy levels is the existence of zero-energy states.

Then, we investigated some of the statistical characteristics of the considered system at high temperatures by comparison of the thermodynamic functions. We found that the fundamental scales of the model have an important role on the thermal quantities. We comprehended that the contribution of the deformation parameter of the de Sitter space-time is more significant than the Snyder model parameter. We also found the influence of SdS model can be seen only at high-temperatures limits.

Acknowledgment: The authors thank the referees for a thorough reading of our manuscript and for constructive suggestion.

Author contribution: All the authors have accepted responsibility for the entire content of this submitted manuscript and approved submission.
Research funding: None declared.
Conflict of interest statement: The authors declare no conflicts of interest regarding this article.

References

[1] S. Mignemi, "Classical and quantum mechanics of the nonrelativistic Snyder model," *Phys. Rev. D*, vol. 84, no. 2, p. 025021, 2011.
[2] S. Mignemi, "Classical and quantum mechanics in the Snyder space," *J. Phys. Conf.*, vol. 343, no. 1, p. 012074, 2012.
[3] S. A. Franchino-Vinas and S. Mignemi, "Worldline formalism in Snyder spaces," *Phys. Rev. D*, vol. 98, no. 6, p. 065010, 2018.
[4] S. Meljanac, S. Mignemi, J. Trampetic, and J. You, "Nonassociative Snyder ϕ^4 quantum field theory," *Phys. Rev. D*, vol. 96, no. 4, p. 045021, 2017.
[5] S. Mignemi, "The Snyder model and quantum field theory," *Ukrainian J. Phys.*, vol. 64, no. 11, p. 991, 2019.
[6] S. A.Franchino-Vinas and S.Mignemi, arXiv:2005.12610.
[7] L. Lu and A. Stern, "Snyder space revisited," *Nucl. Phys. B*, vol. 854, no. 3, p. 894, 2012.
[8] W. S. Chung and H. Hassanabadi, "Modified anti Snyder model with minimal length, momentum cutoff and convergent partition function," *Int. J. Theor. Phys.*, vol. 58, no. 7, p. 2267, 2019.
[9] M. V. Battisti and S. Meljanac, "Modification of Heisenberg uncertainty relations in noncommutative Snyder space-time geometry," *Phys. Rev. D*, vol. 79, no. 6, p. 067505, 2009.
[10] M. V. Battisti and S. Meljanac, "Scalar field theory on noncommutative Snyder spacetime," *Phys. Rev. D*, vol. 82, no. 2, p. 024028, 2010.
[11] H. S. Snyder, "Quantized space-time," *Phys. Rev.*, vol. 71, no. 1, p. 38, 1947.
[12] H. S. Snyder, "The electromagnetic field in quantized space-time," *Phys. Rev.*, vol. 72, no. 1, p. 68, 1947.
[13] C. N. Yang, "On quantized space-time," *Phys. Rev.*, vol. 72, no. 9, p. 874, 1947.
[14] Y. A. Gol'fand, "On the properties of displacements in p-space of constant curvature," *Sov. Phys. JETP*, vol. 17, p. 842, 1963.
[15] V. G. Kadyshevsky, "On the theory of quantization of space-time," *Sov. Phys. JETP*, vol. 14, p. 1340, 1962.
[16] R. M. Mir-Kasimov, ""Focusing" singularity in p-space of constant curvature," *Sov. Phys. JETP*, vol. 22, p. 629, 1966.
[17] Y. A. Gol'fand, "Quantum field theory in constant curvature p-space," *Sov. Phys. JETP*, vol. 16, p. 184, 1963.
[18] R. M. Mir-Kasimov, "The Coulomb field and the nonrelativistic quantization of space," *Sov. Phys. JETP*, vol. 25, p. 348, 1967.
[19] G. Amelino-Camelia, L. Smolin, and A. Starodubtsev, "Quantum symmetry, the cosmological constant and Planck-scale phenomenology," *Classical Quant. Grav.*, vol. 21, no. 13, p. 3095, 2004.
[20] H.-Y. Guo, Yu. C.-G. Huang, Z. X. Tian, and B. Zhou, "Snyder's quantized space-time and de Sitter special relativity," *Front. Phys. China*, vol. 2, no. 3, p. 358, 2007.
[21] J. Kowalski-Glikman and L. Smolin, "Triply special relativity," *Phys. Rev. D*, vol. 70, no. 6, p. 065020, 2004.
[22] S. Mignemi, "Classical and quantum mechanics of the nonrelativistic Snyder model in curved space," *Classical Quant. Grav.*, vol. 29, no. 21, p. 215019, 2012.
[23] S. Mignemi, "Extended uncertainty principle and the geometry of (anti)-de Sitter space," *Mod. Phys. Lett. A*, vol. 25, no. 20, p. 1697, 2010.
[24] W. S. Chung and H. Hassanabadi, "Quantum mechanics on (anti)-de Sitter background," *Mod. Phys. Lett. A*, vol. 32, no. 26, p. 1750138, 2017.
[25] B. Ivetic, S. Meljanac, and S. Mignemi, "Classical dynamics on curved Snyder space," *Classical Quant. Grav.*, vol. 31, no. 10, p. 105010, 2014.
[26] S. A. Franchino-Viñas and S. Mignemi, "Snyder-de Sitter Meets the Grosse-Wulkenhaar Model," In: F. Finster, D. Giulini, J. Kleiner, J. Tolksdorf (eds)., *Progress and Visions in Quantum Theory in View of Gravity*. Birkhäuser, Cham. 2020, https://doi.org/10.1007/978-3-030-38941-3_6.
[27] S. Mignemi, "Doubly special relativity in de Sitter spacetime," *Ann. Phys.*, vol. 522, no. 12, p. 924, 2010.
[28] S. Mignemi, "The Snyder–de Sitter model from six dimensions," *Classical Quant. Grav.*, vol. 26, no. 24, p. 245020, 2009.
[29] S. Mignemi and R. Strajn, "Quantum mechanics on a curved Snyder space," *Adv. High Energy Phys.*, vol. 2016, p. 1328284, 2016.
[30] B. Hamil, M. Merad, and T. Birkandan, "Pair creation in curved Snyder space," *Int. J. Mod. Phys. A*, vol. 35, no. 4, p. 2050014, 2020.
[31] S. A. Franchino-Vinas and S. Mignemi, "Asymptotic freedom for λ ϕ^ 4_ ⋆ λ ϕ⋆ 4 QFT in Snyder–de Sitter space," *Eur. Phys. J. C*, vol. 80, no. 5, p. 382, 2020.
[32] M. Hadj Moussa and M. Merad, "Relativistic oscillators in generalized Snyder model," *Few Body Syst.*, vol. 59, no. 3, p. 44, 2018.
[33] M. Merad and M. Hadj Moussa, "Exact solution of Klein–Gordon and Dirac equations with Snyder–de Sitter algebra," *Few Body Syst.*, vol. 59, no. 1, p. 5, 2018.
[34] M. Falek, M. Merad, and T. Birkandan, "Duffin–Kemmer–Petiau oscillator with Snyder-de Sitter algebra," *J. Math. Phys.*, vol. 58, no. 2, p. 023501, 2017.
[35] H. Hassanabadi, E. Maghsoodi, W. S. Chung, and M. de Montigny, "Thermodynamics of the Schwarzschild and Reissner–Nordström black holes under the Snyder–de Sitter model," *Eur. Phys. J. C*, vol. 79, no. 11, p. 936, 2019.
[36] M. M. Stetsko, "Dirac oscillator and nonrelativistic Snyder-de SITter algebra," *J. Math. Phys.*, vol. 56, no. 1, p. 012101, 2015.
[37] A. K. Geim and K. S. Novoselov, *Nanoscience and Technology: A Collection of Reviews from Nature Journals*, Singapore, World Scientific, 2010.
[38] O. L. Berman, R. Y. Kezerashvili, and K. Ziegler, "Coupling of two Dirac particles," *Phys. Rev. A*, vol. 87, no. 4, p. 042513, 2013.
[39] M. Günay, V. Karanikolas, R. Sahin, R. V. Ovali, A. Bek, and M. E. Tasgin, "Quantum emitter interacting with graphene coating in the strong-coupling regime," *Phys. Rev. B*, vol. 101, no. 16, p. 165412, 2020.

[40] M. Gullans, D. E. Chang, F. H. L. Koppens, F. J. G. de Abajo, and M. D. Lukin, "Single-photon nonlinear optics with graphene plasmons," *Phys. Rev. Lett.*, vol. 111, no. 24, p. 247401, 2013.
[41] K. S. Novoselov, A. K. Geim, S. V. Morozov, et al., "Electric field effect in atomically thin carbon films," *Science*, vol. 306, no. 5696, p. 666, 2004.
[42] Y. Zhang, J. P. Small, M. E. S. Amori, and P. Kim, "Electric field modulation of galvanomagnetic properties of mesoscopic graphite," *Phys. Rev. Lett.*, vol. 94, no. 17, p. 176803, 2005.
[43] Z. Fang, S. Thongrattanasiri, A. Schlather, et al., "Gated tunability and hybridization of localized plasmons in nanostructured graphene," *ACS Nano*, vol. 7, no. 3, p. 2388, 2013.
[44] A. H. Castro Neto, F. Guinea, N. M. R. Peres, K. S. Novoselov, and A. K. Geim, "The electronic properties of graphene," *Rev. Mod. Phys.*, vol. 81, no. 1, p. 109, 2009.
[45] M. A. H. Vozmediano, M. I. Katsnelson, and F. Guinea, "Gauge fields in graphene," *Phys. Rep.*, vol. 496, no. 4–5, p. 109, 2010.
[46] I. S. Gradshteyn and I. M. Ryzhik, *Tables of Integrals, Series and Products*, New York, Academic, 1980.
[47] B. Hamil and M. Merad, "Dirac equation in the presence of minimal uncertainty in momentum," *Few Body Syst.*, vol. 60, no. 2, p. 36, 2019.
[48] C. Bastos, O. Bertolami, N. Dias, and J. Prata, "Noncommutative graphene," *Int. J. Mod. Phys. A*, vol. 28, no. 16, p. 1350064, 2013.
[49] V. Santos, R. V. Maluf, and C. A. S. Almeida, "Thermodynamical properties of graphene in noncommutative phase–space," *Ann. Phys.*, vol. 349, p. 402, 2014.
[50] H. Bateman and A. Erdelyi, *Higher Transcendental Functions*, New York, McGraw-Hill Book Comp, 1953.
[51] Ya. B. Zel'dovich and Yu. P. Raizer, *Physics of Shock Waves and High-Temperature Hydrodynamic Phenomena*, New York, Academic, 1966.
[52] R. Houça and A. Jellal, "Thermodynamic properties of graphene in a magnetic field and Rashba coupling," *Phys. Scripta*, vol. 94, no. 10, p. 105707, 2019.
[53] A. Boumali, "Thermodynamic properties of the graphene in a magnetic field via the two-dimensional Dirac oscillator," *Phys. Scripta*, vol. 90, no. 4, p. 109501, 2015.